Conditional Deletion of *Dnaic1* in a Murine Model of Primary Ciliary Dyskinesia Causes Chronic Rhinosinusitis

Lawrence E. Ostrowski[1,2], Weining Yin[1], Troy D. Rogers[1], Katie B. Busalacchi[1], Michael Chua[3], Wanda K. O'Neal[1], and Barbara R. Grubb[1]

[1]Cystic Fibrosis/Pulmonary Research and Treatment Center; [2]Department of Cell and Developmental Biology; and [3]Department of Cell and Molecular Physiology, The University of North Carolina at Chapel Hill School of Medicine, Chapel Hill, North Carolina

Studies of primary ciliary dyskinesia (PCD) have been hampered by the lack of a suitable animal model because disruption of essential ciliary genes in mice results in a high incidence of lethal hydrocephalus. To develop a viable mouse model for long-term studies of PCD, we have generated a transgenic mouse line in which two conserved exons of the mouse intermediate dynein chain gene, *Dnaic1*, are flanked by loxP sites (*Dnaic1*$^{flox/flox}$). *Dnaic1* is the murine homolog of human *DNAI1*, which is mutated in approximately 10% of human PCD cases. These mice have been crossed with mice expressing a tamoxifen-inducible Cre recombinase (CreER). Treatment of adult *Dnaic1*$^{flox/flox}$/*CreER*$^{+/-}$ mice with tamoxifen results in an almost complete deletion of *Dnaic1* with no evidence of hydrocephalus. Treated animals have reduced levels of full-length Dnaic1 mRNA, and electron micrographs of cilia demonstrate a loss of outer dynein arm structures. In treated *Dnaic1*$^{flox/flox}$/*CreER*$^{+/-}$ animals, mucociliary clearance (MCC) was reduced over time. After approximately 3 months, no MCC was observed in the nasopharynx, whereas in the trachea, MCC was observed for up to 6 months, likely reflecting a difference in the turnover of ciliated cells in these tissues. All treated animals developed severe rhinosinusitis, demonstrating the importance of MCC to the health of the upper airways. However, no evidence of lung disease was observed up to 11 months after *Dnaic1* deletion, suggesting that other mechanisms are able to compensate for the lack of MCC in the lower airways of mice. This model will be useful for the study of the pathogenesis and treatment of PCD.

Keywords: primary ciliary dyskinesia; cilia; mucociliary clearance; bronchiectasis; rhinosinusitis

Mucociliary clearance (MCC) is an important innate defense mechanism of the mammalian lung (1, 2). The cilia, which provide the force for MCC, and the overlying mucous layer, which traps inhaled material, are essential for effective MCC. Impaired MCC is a common feature of many airway diseases and can be the result of environmental exposure to toxins (e.g., cigarette smoke, ozone), pathogens (e.g., bacteria, viruses), or genetic mechanisms. Patients with genetic defects in MCC suffer from repeated episodes of airway infection and eventually develop bronchiectasis. Individuals afflicted with primary ciliary dyskinesia (PCD), an inherited disease caused by mutations that result in defective cilial function, exhibit chronic rhinosinusitis, otitis media, and bronchitis, frequently leading to bronchiectasis (3–6). In cystic fibrosis (CF), mutations in the CF transmembrane conductance regulator (CFTR) protein result in a thick mucus layer that prevents effective MCC and results in the chronic lung disease that causes the majority of mortality associated with this disease (7, 8). The difference in severity of the two genetic diseases has been attributed to the fact that patients with PCD are capable of using cough as an alternative mechanism of clearance, whereas in CF, the thickened mucus is not easily removed even by vigorous coughing. Although MCC and cough are clearly effective in the larger airways, the mechanisms responsible for the clearance of inhaled particles from the respiratory bronchioles and alveoli, which lack ciliated cells, are not well understood.

CLINICAL RELEVANCE

This report describes the development of a viable mouse model for the human disease primary ciliary dyskinesia. The model will be useful for studies of the pathogenesis and treatment of this and other airway diseases and for basic studies of ciliary biology and airway clearance.

To investigate the role of MCC and other clearance mechanisms in lung defense, it would be useful to have an animal model in which MCC has been eliminated by inactivation of the cilia. However, the inactivation of MCC by targeted deletion of essential ciliary genes using standard knock-out procedures (9–11), or the random inactivation of ciliary genes by other techniques (12–16), usually results in mice with severe developmental defects, including hydrocephalus and situs ambiguities (15, 17). Thus, although these animals lack MCC, they typically die from other causes before reaching adulthood and are largely unsuitable for studying the role of MCC in the prevention of airway disease.

To develop a model of PCD that replicates features of the human disease without the high incidence of hydrocephalus and other developmental abnormalities, we have generated a mouse model carrying an inducible deletion in a gene coding for an intermediate dynein chain, *Dnaic1*. *Dnaic1* is the murine homolog of the human gene *DNAI1* that is mutated in approximately 10% of patients with PCD (18–21). The DNAI1 protein is a component of the outer dynein arm (ODA), and mutations in this protein frequently result in the absence of the ODA, as visible by electron microscopy. By allowing animals homozygous for the conditional deletion to survive the neonatal period before inducing the deletion in *Dnaic1*, we hypothesized that animals with impaired MCC suitable for long-term studies could be obtained in the absence of hydrocephalus or other developmental abnormalities.

Our data demonstrate that the Cre-mediated deletion of the *Dnaic1* gene occurs with high efficiency and results in the loss of ODA structures in respiratory cilia. The absence of the ODA results in ciliary immotility *in vitro* and in the absence of MCC *in vivo*. Animals treated to induce the deletion of *Dnaic1* have survived for up to 11 months with no evidence of hydrocephalus.

(*Received in original form April 6, 2009 and in final form June 30, 2009*)

This work was supported by NIH grants HL084328 and P30 DK065988 and the Cystic Fibrosis Foundation grant R026-CR07.

Correspondence and requests for reprints should be addressed to Lawrence E. Ostrowski, The University of North Carolina at Chapel Hill School of Medicine, Cystic Fibrosis/Pulmonary Research and Treatment Center, CB# 7248, 6123A Thurston-Bowles Bldg., Chapel Hill, NC 27599-7248. E-mail: ostro@med.unc.edu

This article has an online supplement, which is accessible from this issue's table of contents at www.atsjournals.org

Am J Respir Cell Mol Biol Vol 43. pp 55–63, 2010
Originally Published in Press as DOI: 10.1165/rcmb.2009-0118OC on August 12, 2009
Internet address: www.atsjournals.org

These animals develop severe rhinosinusitis, consistent with a PCD phenotype. This model should be useful for studies of the pathogenesis and treatment of PCD and other airway diseases.

MATERIALS AND METHODS

General

RNA and DNA were isolated using RNeasy and DNeasy kits (Qiagen Inc., Valencia, CA) according to the manufacturer's protocols. Routine genotyping and analysis were performed using AmpliTaq Gold (Applied Biosystems, Foster City, CA) or REDExtract-N-Amp kit (Sigma-Aldrich, St. Louis, MO) and an Applied Biosystems thermocycler with primers that span the targeted region (primers are listed in Table E1 in the online supplement). Quantitative PCR to determine the amount of intact *Dnaic1* remaining after tamoxifen treatment was performed using LightCycler SYBR Green reagents (Roche Applied Science, Mannheim, Germany) and a Roche LightCycler using primers that were internal to the deleted region.

Generation of *Dnaic1$^{flox/flox}$* Transgenic Animals

Briefly, high-fidelity, long-distance PCR (Takara Bio, Madison, WI) was used to amplify fragments of mouse genomic DNA surrounding exons 17 and 18 of *Dnaic1*. The fragments were cloned into a plasmid containing the flanking loxP sites and selectable markers. The plasmid construct was electroporated into ES cells, and neomycin-resistant clones were screened by Southern analysis. The neomycin cassette was flanked by FRT sites and was removed using FLP recombinase. The selected ES cells were injected into mouse blastocysts and transferred to pseudo-pregnant female mice to allow for development of transgenic mice carrying the targeted *Dnaic1* gene. Mice were genotyped by PCR of genomic DNA using primers that flank the targeted region. All animal procedures were approved by the UNC IACUC committee.

Breeding and Tamoxifen Treatment

Dnaic1$^{flox/flox}$ animals were maintained on a mixed background (C57Bl6/129) and were mated to mice expressing a tamoxifen-inducible Cre recombinase under control of the Rosa promoter (R26CreER; Jackson Laboratory, Bar Harbor, ME [22]). Typically, we mated *Dnaic1$^{flox/flox}$/CreER$^{-/-}$* mice with *Dnaic1$^{wt/flox}$/CreER$^{+/+}$* to generate experimental animals. Tamoxifen (Sigma-Aldrich) was dissolved in pure corn oil at 10 mg/ml (23). For all studies, *Dnaic1$^{flox/flox}$/CreER$^{+/-}$* were treated with tamoxifen (five intraperitoneal injections of 75 μg/g body weight) to generate PCD animals. In most experiments, PCD animals were compared with *Dnaic1$^{wt/flox}$* or *Dnaic1$^{wt/wt}$* that were also treated with tamoxifen. In early studies, we found that treating younger animals (3–4 wk of age) or administering the tamoxifen treatment on consecutive days caused intestinal pathology and death in the CreER transgenic mice (independent of *Dnaic1* status); therefore, in later studies older animals were studied (~8–12 wk of age), and tamoxifen was administered every 2 to 3 days. We also observed some "leakiness" of the CreER transgene (i.e., deletion of the targeted allele in the absence of tamoxifen treatment).

Tracheal Cell Culture

Mouse tracheal epithelial cells were cultured at an air–liquid interface on 12-mm collagen-coated Millicell-CM culture inserts (0.4 μm pore) (Millipore Corp., Billerica, MA) essentially as previously described (24). Ciliary activity was visualized using phase contrast microscopy and measured using the SAVA program (25) to analyze nine different low-magnification fields (one central, eight peripheral) from each insert. For treatment of cultures, tamoxifen was dissolved in ethanol at 10 mM and diluted in media to a final concentration of 1 μM. Tamoxifen was added at the time of plating and with each media change for the first 5 to 6 days of culture. Control cultures were treated with an equal volume of ethanol.

Generation of a Monoclonal Antibody against Dnaic1 and Western Blotting

Monoclonal antibodies against Dnaic1 were produced by immunization of mice with the peptide RGTRKRDEDSGTEVGEGTDEC from the amino terminal of the human DNAI1 protein. All immunization and screening protocols were performed by the UNC Immunology Core Facility using standard procedures. For selection of hybridomas, isolated human ciliary axonemes (26) were analyzed by Western blotting. Additional screenings were performed using a murine Dnaic1-EGFP fusion protein expressed in 293 cells. For analysis of mouse tracheal epithelial cells, total cell lysates were prepared in Mammalian Protein Extraction Reagent (Pierce, Rockford, IL). Ciliary axonemes were isolated from cultured mouse tracheal epithelial cells as previously described (26) and prepared in gel-loading buffer. Protein samples were fractionated on 4 to 12% Bis-Tris gradient gels (Invitrogen, Carlsbad, CA), transferred to nitrocellulose membranes, and probed using Amersham ECL Plus reagents (GE Healthcare, Buckinghamshire, UK), all according to manufacturers instructions.

Quantification of *Dnaic1* by PCR

Genomic DNA was isolated from mouse tissues (tail, lung, or trachea) using the DNeasy Kit according to the manufacturers' instructions (Qiagen).

DNA concentrations were determined by spectrophotometry. Real-time PCR was performed using a Roche Lightcycler 4.0 and the Lightcycler FastStart DNA Master SYBR green I kit (Roche Applied Science). Primers specific to exons 17 and 18 were used to analyze the amount of intact *Dnaic1* (*see* Table E1 in the online supplement). Each sample was analyzed in duplicate. Relative changes in the level of intact *Dnaic1* (wild-type remaining) were calculated from the efficiency of the PCR reaction and the cross-point deviation between samples of *Dnaic1$^{flox/flox}$*, *Dnaic1$^{wt/flox}$* and their wild-type littermate control animals and determined by normalization to the reference gene β-ENaC (*Scnn1b*) (27).

Measurement of Mucociliary Clearance in the Nasopharynx

To determine the rate of clearance of endogenous mucus from the upper airways, animals were killed by CO_2 asphyxiation, and the lower jaw was removed. Using a sharp scalpel, an incision was made through the skin and fascia over the most caudal palatine fold (for an illustration of the relevant mouse anatomy, *see* Ref. 28). The skin and fascia were carefully removed from the soft palate by peeling the tissue caudally using fine forceps. Once the skin and fascia were removed from the soft palette, the very thin ventral wall of the nasopharyngeal (NP) meatus was evident, and the beating cilia were clearly seen clearing debris caudally. The beginning of Video 1 in the online supplement shows the palatine ridges of the hard palate and upper molars to the right side, with the exposed NP cavity in the middle of the field. Water-equilibrated mineral oil was applied to the membrane to prevent desiccation. Because the cilia are on the opposite side of the membrane (and the NP cavity is not actually opened), the mineral oil does not contact the cilia. The entire process can be completed in less than 5 minutes, and MCC can usually be visualized for up to 30 minutes after death. For image acquisition, the preparation was placed under a dissecting scope. A video camera (MTI, Michigan City, IN) was mounted on the scope and interfaced with a VHS recorder and monitor. Before MCC was recorded, a slide micrometer was placed on the stage of the dissecting scope to calibrate distance measurements. Once the video was recorded, MCC was determined by playing the video back and determining the time it took particles to traverse a calibrated distance (corresponding to an *in vivo* distance of 0.5–1 mm) on the monitor screen. Usually, 5 to 10 particles were measured, and the average MCC was calculated as mm/min by an investigator blinded to the animals' genotype. For each time point, the rate of MCC is expressed as a percentage of the control animals studied under the same conditions at the same time point.

Measurement of Mucociliary Transport in the Trachea

For these studies, we used a modification of previously described techniques (29, 30). Animals were anesthetized with a mixture of ketamine/xylazine (90 and 10 mg/kg body weight, respectively), and the trachea was surgically exposed (not opened). The mouse was then killed by exsanguination. Using a fine-bore cannula, approximately 500 nl of 0.2% low-melting point agarose containing fluorescent microspheres (1 μm Molecular Probes FluoSpheres, Nile Red; Invitrogen Corp., Carlsbad, CA) were deposited via the epiglottis in the closed

trachea near the bifurcation. The mouse was positioned with the head elevated approximately 10°, and the transport of the fluorescent beads was recorded using a Leica MZ 16FA fluorescent dissecting microscope and a digital camera. The rate of MCC was determined by measuring the time required for fluorescent particles to move a measured distance by an investigator blinded to the animals' genotype. Usually, 5 to 10 particles were measured for each animal, and the average was taken as the rate of MCC. For each time point, the rate of MCC is expressed as a percentage of the control animals studied under the same conditions at the same time point.

Histology Procedures

After the measurement of MCC by the above methods, the head was removed, skinned, and fixed in 10% buffered formalin.

After acid decalcification (~ 24 h), paraffin sections were prepared at three different levels of the nasal cavity: one in front of the incisive papilla, one at the level of the second palatal ridge, and one at the level of the third molar (~ 6, 11, and 28, based on Ref. 31). Sections were stained with hematoxylin and eosin, alcian blue–periodic acid Schiff (to visualize mucus accumulation), and alcian yellow–toulidine blue (to visualize neutrophils and bacteria). For comparisons between groups, the middle section of each sample was scored from 0 to 4 for the presence of mucus, neutrophils, and degeneration of the epithelium, according to the criteria in Figure E1 in the online supplement. Additional sections were prepared from the mid-brain region and examined for evidence of hydrocephalus. Typically, a sample of tissue was taken from the left lung for DNA and RNA analysis, and the four right lung lobes were fixed by immersion in 4% paraformaldehyde and stained as described above.

Transmission Electron Microscopy

Tracheal tissue was fixed in fresh 2% paraformaldehyde and 2% glutaraldehyde with 0.5% tannic acid and processed for transmission electron microscopy. Images were obtained on a Zeiss 900 TEM at a magnification of 50,000, and 8 × 10-inch glossy photographs were prepared. Counts of ODAs were obtained from cilia that were in the plane of focus (with the central pair and radial spokes visible), and one or two cilia were counted from each image. Image averaging of individual microtubule doublets was performed as previously described (32).

RESULTS

Design of Targeting Construct

To generate a murine model of PCD that closely resembles the human disease, we targeted the murine homolog of the human ODA intermediate chain, DNAI1. Mutations in DNAI1 occur in approximately 10% of patients with PCD, and these patients exhibit all the features of classic PCD, including otitis media, chronic rhinosinusitis, bronchiectasis, low levels of nasal nitric oxide, and situs inversus (19). In addition, all of these patients demonstrate an almost complete absence of ODAs in respiratory cilia examined by electron microscopy. The murine Dnaic1 protein (NP_780347) is 82% identical to the human DNAI1 protein (NP_036276), with a high degree of similarity throughout the molecule, including several conserved tryptophan-aspartate repeat sequences (WD repeats) that mediate protein–protein interactions (33). Analysis of *Dnaic1* expression by RT-PCR of various mouse tissues confirmed that murine *Dnaic1* is highly expressed in tissues that contain cilia or flagella (e.g., trachea, nasal epithelium, and testis) but show little or no expression in tissues without cilia (e.g., spleen, muscle) (Figure 1). These data strongly suggested that *Dnaic1* was a suitable target for generating a murine model of PCD. To avoid the high incidence of neonatal hydrocephalus that occurs in traditional knock-outs of ciliary genes, we used the Cre-lox system to target the *Dnaic1* gene for inducible deletion (23). Many of the mutations that cause PCD occur in the WD repeat region, including point mutations that remove a single tryptophan residue at position 568 in one of the WD repeats (19). These WD repeats, which are conserved in the murine protein, are likely involved in the assembly of the ODAs (33). Based on sequence analysis and comparison to the human gene, we have targeted exons 17 and 18 for deletion from the *Dnaic1* gene (Figure 2) by inserting flanking loxP sequences (*Dnaic1*^{flox}). This in-frame deletion is predicted to remove 83 amino acids and completely remove one of the highly conserved WD repeat regions, including the tryptophan residue corresponding to position 568 in human DNAI1.

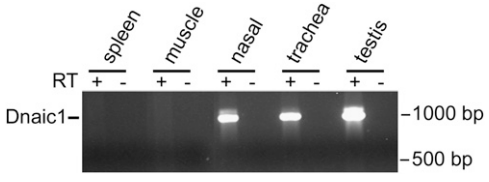

Figure 1. Expression of *Dnaic1* mRNA in various mouse tissues. RT-PCR was performed on RNA isolated from the indicated tissues using primers specific for *Dnaic1* mRNA. A strong positive signal was obtained from tissues with cilia (trachea, nasal) and flagella (testis); other tissues were negative.

Transgenic animals carrying the correctly targeted *Dnaic1* gene were obtained by standard techniques and verified by sequencing (*see* MATERIALS AND METHODS). To induce a PCD phenotype in the respiratory system, it was desirable to induce the *Dnaic1* deletion in essentially all ciliated cells of the upper and lower airways. To achieve the highest percentage of Cre-mediated deletion as possible, the *Dnaic1*^{flox} mice generated above were crossed with a transgenic line expressing high levels of a tamoxifen-activated Cre recombinase under control of the ubiquitous Rosa26 promoter (RosaCreER; Jackson Laboratory).

Effect of Dnaic1 Deletion *In Vitro*

To determine the effect of the Cre-mediated deletion of *Dnaic1* on ciliary activity, tracheal epithelial cells were isolated from *Dnaic1*$^{flox/flox}$ mice that were heterozygous for the Rosa/CreER (Cre$^{+/-}$) transgene. Control cells were isolated from *Dnaic1*$^{wt/wt}$ mice that were also Cre$^{+/-}$. The cells were plated on collagen coated inserts in the presence or absence of 1 μM tamoxifen for the first 6 days of culture. PCR analysis of genomic DNA

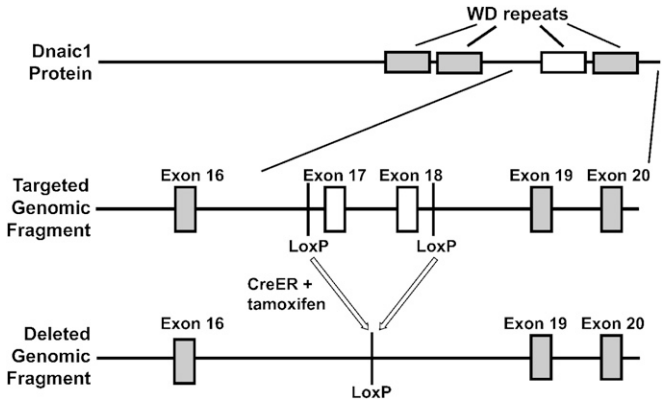

Figure 2. Schematic diagram of the *Dnaic1* protein (*top*) showing the approximate location of the WD repeats. Diagram of the targeted genomic region of *Dnaic1* (*middle*) showing the loxP sites flanking exons 17 and 18. These exons include one of the WD repeat regions. Activation of CreER with tamoxifen causes the removal of exons 17 and 18 (*bottom*).

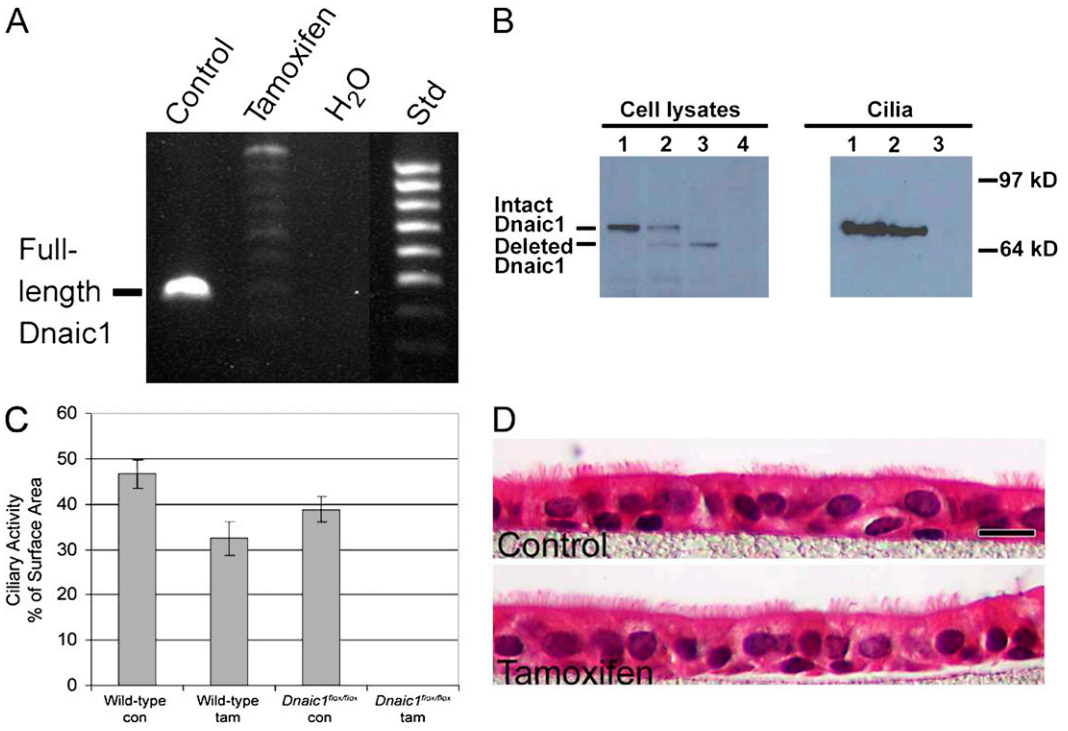

Figure 3. (*A*) Genomic DNA was isolated from untreated cultures of homozygous loxP/*Dnaic1* (control) or from cultures treated for 6 days with tamoxifen and amplified with primers specific to exons 17 and 18. The tamoxifen-treated cultures demonstrate an almost complete absence of full-length *Dnaic1*. In the tamoxifen-treated culture, the absence of a specific target results in the generation of some nonspecific products. (*B*) Western blot analysis of Dnaic1 expression in mouse tracheal cells (*left panel*). Total cell lysates from differentiated cultures of wild-type (WT) (*lane 1*), *Dnaic1*$^{flox/Wt}$ (*lane 2*), *Dnaic1*$^{flox/flox}$ (*lane 3*), and undifferentiated WT (*lane 4*) mouse tracheal epithelial cells were separated by gel electrophoresis and probed with a monoclonal antibody against Dnaic1. Cultures from WT mice express only the full length Dnaic1 protein; cultures of *Dnaic1*$^{flox/flox}$ cells express only the shorter, deleted protein. Heterozygote cultures (*Dnaic1*$^{flox/Wt}$) express both products; undifferentiated cells express neither. Cilia isolated from cultures of WT (*right panel*, *lane 1*) and *Dnaic1*$^{flox/Wt}$ (*lane 2*) cultures show clear incorporation of the full-length protein, whereas cilia isolated from *Dnaic1*$^{flox/flox}$ cells show no incorporation of the deleted Dnaic1 protein (*lane 3*). (*C*) Ciliary activity in cultures of WT and *Dnaic1*$^{flox/flox}$ mouse tracheal epithelial cells treated with tamoxifen or vehicle control. All cultures were positive for the CreER transgene. Cultures were treated for the first 6 days of culture, and ciliary activity was measured on Day 20. Control cultures averaged greater than 30% ciliated surface area, whereas the PCD cultures averaged less than 1%. Data shown are from one representative experiment with three cultures in each group and nine measurements per culture ($n = 27$ for each condition). *Error bars* indicate SEM. (*D*) Hematoxylin and eosin–stained paraffin section of *Dnaic1*$^{flox/flox}$ mouse tracheal epithelial cells cultured in the absence (*top*) or presence (*bottom*) of 1 μM tamoxifen. Fully differentiated ciliated cells are abundant in both cultures. Images are representative of two independent experiments.

yielded almost undetectable amounts of intact *Dnaic1* in the tamoxifen-treated *Dnaic1*$^{flox/flox}$ cultures (Figure 3A). Analysis of total cellular proteins by Western blotting with a monoclonal antibody against Dnaic1 (Figure 3B, *left panel*) demonstrates the production of the full-length Dnaic1 protein in the *Dnaic1*$^{wt/wt}$ cultures (*lane 1*), whereas only the smaller, deleted Dnaic1 protein is detectable in the *Dnaic1*$^{flox/flox}$ cultures (*lane 3*). Both the full-length and the deleted protein are present in lysates from heterozygous cultures (*lane 2*), suggesting that the deleted protein is stable. As expected, undifferentiated (nonciliated) cultures do not express detectable Dnaic1 (*lane 4*). Ciliary axonemes (Figure 3B, *right panel*) isolated from *Dnaic1*$^{wt/wt}$ and *Dnaic1*$^{wt/flox}$ cultures show only the full-length Dnaic1 protein (*lanes 1* and *2*), and ciliary axonemes from the *Dnaic1*$^{flox/flox}$ cultures show no incorporation of the deleted protein (*lane 3*). These results clearly show that the full-length Dnaic1 is preferentially incorporated into the cilia of the heterozygote cultures, whereas the deleted Dnaic1 is incapable of being correctly assembled into the ODA. After 10 days of culture, the surfaces of the control cultures were covered with easily visible, actively beating cilia, whereas only a few actively beating cilia were observed in the tamoxifen-treated *Dnaic1*$^{flox/flox}$ cultures. To determine the percentage of the culture surface covered with actively beating cilia, video microscopy and computer analysis were used to determine the area of each field that contained actively beating cilia. Almost half of the surface of untreated control (WT) cultures exhibited ciliary activity (46.6%), whereas untreated cultures from *Dnaic1*$^{flox/flox}$ mice averaged 38.8% (Figure 3C). Activation of CreER by tamoxifen treatment had a modest effect on ciliary activity in the WT cultures, reducing the percentage of ciliated surface area to 32.4%. In contrast, tamoxifen treatment of the *Dnaic1*$^{flox/flox}$ cultures resulted in an almost complete inhibition of ciliary activity (<1.0%). To further confirm that the tamoxifen treatment was not having a cytotoxic effect or inhibiting ciliated cell differentiation, paraffin sections were prepared and stained with hematoxylin and eosin at the conclusion of the experiment. Ciliated cells were clearly visible throughout both cultures (Figure 3D), and there was no obvious difference between the control and the tamoxifen-treated culture in the appearance of the epithelium or the number of ciliated cells.

The above studies demonstrate that the Cre-mediated deletion of the targeted exons in *Dnaic1* is highly efficient in culture and results in an almost complete inhibition of ciliary activity in cultures homozygous for the targeted *Dnaic1* allele.

Dnaic1 Deletion Is Efficient *In Vivo*

To confirm that the tamoxifen treatment chosen (five intraperitoneal injections of 75 μg/g; *see* MATERIALS AND METHODS) was sufficient to induce the deletion of *Dnaic1 in vivo*, genomic DNA was isolated from tail snips of *Dnaic1*$^{flox/flox}$ Cre+/− animals before and after treatment with tamoxifen. Comparison of the genomic DNA samples used for genotyping (before tamoxifen) with the samples isolated several days after tamoxifen treatment by PCR amplification and agarose gel analysis

clearly demonstrated Cre-mediated deletion of the loxP targeted *Dnaic1* gene (not shown). The level of intact Dnaic1 remaining after tamoxifen treatment (measured by Q-PCR on tail snips) was almost always less than 15% (average, 10.9 ± 1.4%; $n = 23$ animals from five experiments). To further confirm that the deletion was occurring in the primary target tissue, genomic DNA was also isolated from the trachea or a portion of the left lung lobe at the conclusion of some studies. PCR analysis demonstrated the expected pattern of products from *Dnaic1*$^{wt/wt}$, *Dnaic1*$^{wt/flox}$, and *Dnaic1*$^{flox/flox}$ animals (Figure 4A), and Q-PCR using primers specific for the intact *Dnaic1* indicated at least 85% deletion in most animals (87.3 ± 1.3%; $n = 15$ animals from three experiments; Table E2).

Analysis of RNA isolated from lung tissue of treated animals also showed the expected distribution of RT-PCR products, with heterozygous animals expressing both the WT and deleted alleles and tamoxifen-treated homozygous animals expressing almost exclusively the deleted allele (Figure 4B).

After treatment with tamoxifen, *Dnaic1*$^{flox/flox}$ animals appeared normal and gained weight at the same rate as control animals. None of the animals displayed physical or behavioral traits associated with hydrocephalus (e.g., doomed heads, lack of appetite, ataxia). Examination of histological sections from the mid-brain region of two groups of animals ($n = 7$) at the conclusion of the experiments (7 and 11 mo after tamoxifen treatment) showed no indication of enlarged ventricles (not shown). These data are consistent with the hypothesis that the development of hydrocephalus due to ciliary dysfunction occurs during early postnatal brain development (17).

To determine if the deletion of exons 17 and 18 from *Dnaic1* would result in ultrastructural defects in the ciliary axoneme, tracheas were isolated from animals 7 months after tamoxifen treatment and analyzed by transmission electron microscopy. Cilia from control mice (Figure 5A) showed the typical 9+2 pattern of microtubule doublets, with inner and ODAs present on most cilia. In contrast, cilia from tamoxifen-treated *Dnaic1*$^{flox/flox}$ mice demonstrated an almost complete lack of outer dynein arms (Figure 5B). The average number of ODAs visible per cilium in control animals was 8.3 ±0.3 ($n = 21$ cilia from three animals), whereas cilia from the PCD mice averaged 1.2 ± 0.8 ODA per cilium ($n = 14$ cilia from two animals). The absence of ODA in the *Dnaic1*$^{flox/flox}$ mice can be more clearly seen in the images obtained by using computer-assisted analysis to average individual microtubule doublets from several different cilia (Figures 5C and 5D) (32).

Dnaic1 Deletion Inhibits Mucociliary Clearance

To generate animals with a PCD phenotype in the absence of hydrocephalus, animals were not treated with tamoxifen until the age of 1 to 3 months, which is beyond the critical time period for the development of hydrocephalus in other PCD models (17). However, at the time of tamoxifen treatment, all animals would already possess a full complement of functional ciliated cells, and the activation of Cre recombinase was not expected to immediately result in a PCD phenotype. To determine the time necessary for the deletion of *Dnaic1* on the genomic level to result in a loss of ciliary function, groups of *Dnaic1*$^{flox/flox}$ mice that were also Cre$^{+/-}$ and control animals were treated with tamoxifen and studied at various times after treatment. As a measure of mucociliary clearance in the upper airways, we have developed a technique in which the transport of endogenous mucus particles in the nasopharynx is quantified. This method allows visualization and quantification of the rate of transport of endogenous mucus particles in the closed nasopharynx, without the addition of exogenous particles or fluid. In control animals, vigorous MCC can be observed for periods longer than 10 minutes (Video 1). Six groups of animals

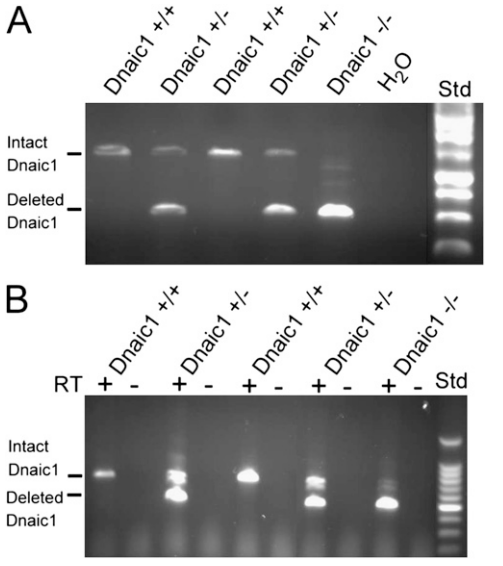

Figure 4. (*A*) Genomic DNA isolated from lung tissue of tamoxifen treated mice was amplified by PCR using primers that span the loxP targeted region of *Dnaic1*. DNA from WT mice (*Dnaci1*$^{+/+}$) produced only the expected 1.4 kb full-length product, DNA from the homozygous loxP/*Dnaic1* mouse (*Dnaic1*$^{-/-}$) produced essentially only the deleted 564 bp product, and samples from the heterozygous mice (*Dnaic1*$^{+/-}$) produced both. (*B*) RNA isolated from the same tissue as in *A* was analyzed by RT-PCR. Note the almost complete absence of intact Dnaic1 mRNA in the homozygous treated animal (*Dnaic1*$^{-/-}$).

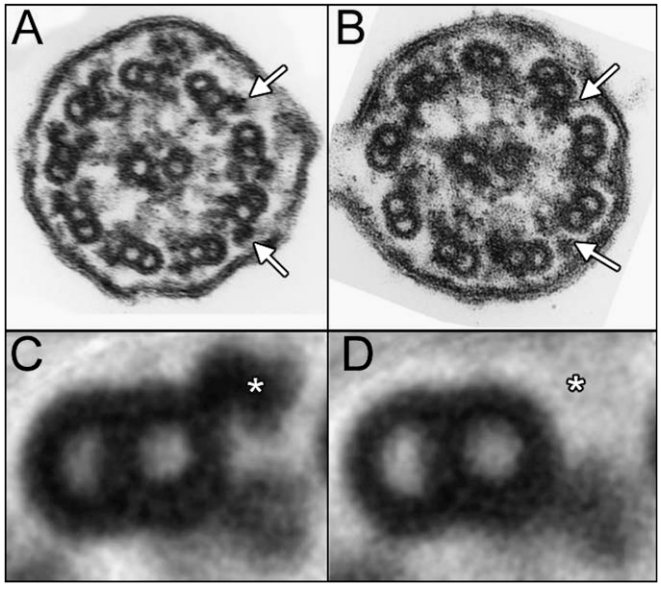

Figure 5. Transmission electron micrographs of tracheal cilia from (*A*) a control mouse (*Dnaic1*$^{wt/flox}$) and (*B*) a mouse with primary ciliary dyskinesia (PCD) (*Dnaic1*$^{flox/flox}$) 7 months after tamoxifen treatment. Outer dynein arms (ODAs) are clearly visible in cilia from the control animal but are absent in cilia from the PCD mouse (*arrows*). Computer-assisted image averaging of individual outer doublets more clearly illustrates the presence of the ODA in control axonemes (*asterisk* in *C*) and the absence of ODA in PCD axonemes (*asterisk* in *D*). Images shown are the average of 17 and 27 doublets, respectively.

were treated with tamoxifen and studied at different times after treatment ($n = 52$). One month after treatment with tamoxifen, several of the *Dnaic1*$^{flox/flox}$ animals displayed substantial rates of MCC (~20–60% of control), whereas three of seven animals examined demonstrated no measurable clearance (Figure 6A). The average rate of MCC in the *Dnaic1*$^{flox/flox}$ animals was 1.3 ± 0.6 mm/min ($n = 7$), significantly different from the control value of 8.9 ± 1.7 mm/min ($n = 8$; $P = 0.001$). Two months after tamoxifen treatment, three of four animals examined showed no MCC in the nasopharynx, and the remaining animal exhibited a drastically reduced rate (1.9 mm/min compared with 10.2 ± 1.2 mm/min for control mice; $n = 8$). All animals examined at 3 months and eight of nine animals examined at longer time periods (up to 11 mo) after tamoxifen treatment demonstrated no MCC in the nasopharynx (Video 2 in the online supplement and data not shown). These results indicate that 2 to 3 months after deletion of the *Dnaic1* gene, MCC is no longer effective in the nasopharynx.

In preliminary studies of the trachea, we observed a substantial amount of ciliary activity in tamoxifen-treated *Dnaic1*$^{flox/flox}$ animals up to 3.5 months after treatment, unlike the absence of MCC in the nasopharynx. To quantify MCC in the lower airways, we used a modification of several previously described techniques. Animals were killed, and, after surgically exposing the trachea, fluorescent microspheres were introduced into the lower trachea via the epiglottis using a catheter. Transport of the fluorescent microspheres was then recorded *in situ* using a fluorescent dissecting microscope. Three groups of animals ($n = 28$) were treated with tamoxifen, and MCC in the trachea was measured at various time points. As expected, all control animals readily transported the particles in a cephalic direction for several minutes, although clearance in the trachea was not as

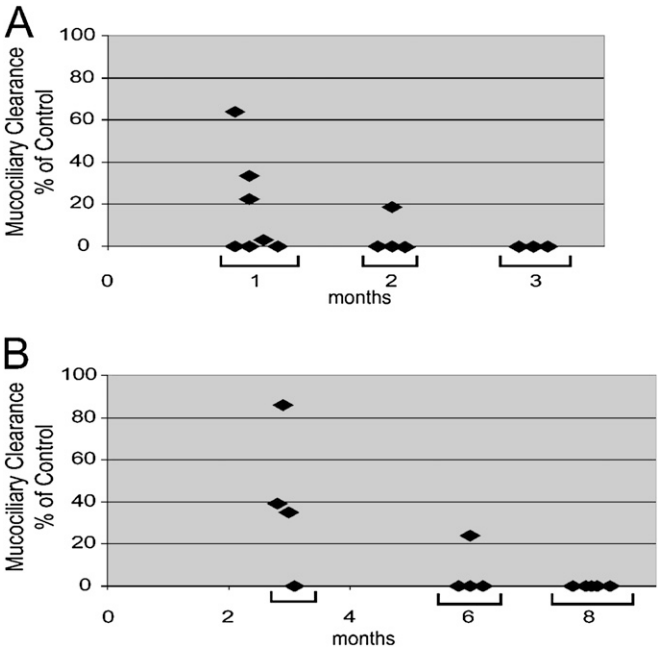

Figure 6. Mucociliary clearance (*A*) in the nasopharynx and (*B*) in the trachea of tamoxifen-treated *Dnaic1*$^{flox/flox}$ mice. Groups of animals were treated with tamoxifen, and mucociliary clearance (MCC) was measured at the times indicated and expressed as a percentage of the rate of MCC in a parallel group of control animals. Complete inhibition of MCC requires approximately 2 months in the nasopharynx and approximately 6 months in the trachea after the deletion of *Dnaic1*. *x* axis = time after tamoxifen treatment in months. Each symbol represents a single animal.

robust as observed in the nasopharynx. Three months after tamoxifen treatment, three of four *Dnaic1*$^{flox/flox}$ animals clearly exhibited active MCC in the trachea (Video 3 in the online supplement illustrates a *Dnaic1*$^{flox/flox}$ animal with clearance; Video 4 is from the animal with no clearance), although the rate of clearance was reduced approximately 50% compared with control animals (1.1 ± 0.5 versus 2.7 ± 0.6 mm/min; $P = 0.04$; $n = 4$) (Figure 6B). Six months after tamoxifen treatment, three of four *Dnaic1*$^{flox/flox}$ mice had no visible MCC, whereas one animal exhibited a substantially reduced rate of clearance. By 7.5 months, none of the *Dnaic1*$^{flox/flox}$ animals exhibited MCC. These results demonstrate that the deletion of exons 17 and 18 of the *Dnaic1* gene in adult mice results in a loss of MCC in both the upper and lower airways but that the loss of MCC in the nasopharynx occurs more quickly, possibly reflecting a faster turnover rate of cilia or ciliated cells in the upper airways.

Deletion of Dnaic1 Causes Chronic Rhinosinusitis

We examined the nasal cavity of tamoxifen-treated *Dnaic1*$^{flox/flox}$ animals to determine if the deletion of *Dnaic1* and the subsequent loss of MCC resulted in pathological changes. All of the animals that had a complete inhibition of MCC in the nasopharynx demonstrated obvious mucus accumulation in the nasal cavity (Figure 7) regardless of the time at which they were studied, whereas no mucus was observed in any of the control animals. Mucus accumulation was clearly present in the nasal cavity, the maxillary sinuses, or the region of the ethmoturbinates. Most animals had large amounts of mucus in the region of the ethmoturbinates, although the specific sites of mucus accumulation varied between animals (Figures 7B and 7C) (34). Some of the mucus-filled areas contained large numbers of infiltrating neutrophils (Figures 7B, 7E, and 7G), whereas other areas contained few or no neutrophils (Figures 7C and 7I). Routine examination of paraffin sections stained with alcian-yellow toulidine blue did not reveal the presence of bacterial colonies. The nasal epithelium was frequently abnormal near the sites of mucus accumulation, with a loss of normal differentiated epithelial cells and a thinning of the lamina propria being the most common findings. Evaluation of PCD animals at different times after treatment revealed no clear trends in the extent of mucus accumulation, numbers of neutrophils, or tissue degeneration (Figure E1). However, the amount of epithelial damage seemed to increase with time after treatment, with animals examined at early time points (1–3 mo) showing some areas of normal epithelium in areas of mucus accumulation and animals examined at later time points (6–11 mo) possessing only a thin layer of undifferentiated cells over much of the dorsal meatus and nasal turbinates (Figure 7I). Many of the ethmoturbinates were severely atrophic, with loss of the surface epithelium, the basal lamina, and the underlying bone (Figure 7I).

In contrast to the nasal cavity, examination of the lungs of tamoxifen-treated *Dnaic1*$^{flox/flox}$ animals revealed no mucus accumulation at any time point (data not shown). In many of the older animals examined (>6 mo), foci of infiltrating lymphocytes were observed; however, the size and incidence of these lesions appeared similar between the *Dnaic1*$^{flox/flox}$ animals and the control animals. Therefore, even in mice with no measurable MCC for approximately 5 months and significant mucus accumulation in the nasal cavity, the lower airways showed no evidence of mucus accumulation or infection.

DISCUSSION

Studies of the pathogenesis and treatment of PCD have been limited, in part due to the small number of patients afflicted with this disease and in part due to the lack of a suitable animal

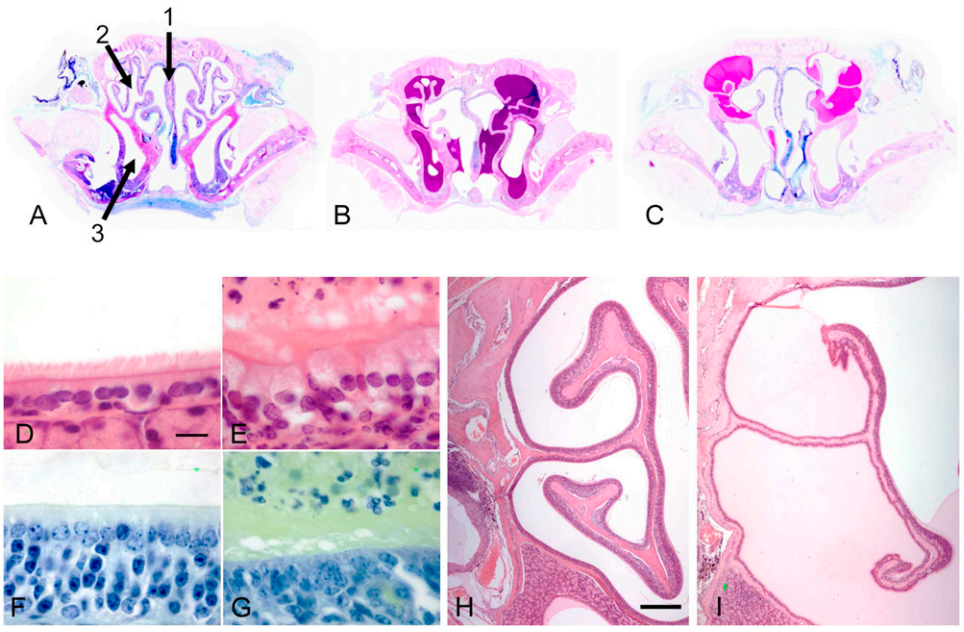

Figure 7. Rhinosinusitis in PCD mice. (*A*) Paraffin section of a control mouse (11 mo) showing the nasal septum (*1*), the ethmoturbinates (*2*), and the maxillary sinus (*3*). Nasal cavity of representative PCD mice 2 (*B*) and 11 (*C*) months after *Dnaic1* deletion. Higher magnification images of ciliated epithelium from the maxillary sinus (*D*, *E*) and olfactory epithelium (*F*, *G*) of a control (*D*, *F*) and of the PCD mouse (*E*, *G*) shown in *B*. Note the accumulation of mucus and inflammatory neutrophils and the degeneration of the epithelium in the PCD animal. (*H* and *I*) Low-magnification images of the ethmoturbinates from the animals shown in *A* and *C*, showing the attenuation of epithelium and the underlying bone structure in the PCD mouse. *A*, *B*, and *C* were stained with alcian blue–periodic acid Schiff; *D*, *E*, *H*, and *I* were stained with hematoxylin and eosin; *F* and *G* were stained with alcian blue–toluidine yellow. *Scale bars* for *D*, *E*, *F*, and *G* = 10 μm; *scale bars* for *H* and *I* = 40 μm.

model. Although canids with PCD are occasionally reported in the literature (35), the time and expense involved has prevented the development of a canine model. Recent interest in the expanding roles of cilia in development and disease processes has led to the development of several mouse lines carrying deletions of genes involved in ciliary structure and function; however, if these genes affect motile cilia function in the ependymal cells, many of the null animals develop hydrocephalus during the neonatal period and die (9, 10, 13–17). In addition, deletion of essential ciliary genes often results in other developmental abnormalities, including congenital heart defects (15). Therefore, these models are not well suited for long-term studies of airway disease caused by PCD or other disorders of mucociliary clearance. In this work, we have developed and characterized a genetically modified mouse strain that carries a conditional loxP targeted deletion in the dynein intermediate chain gene *Dnaic1*. Deletion of exons 17 and 18 of the Dnac1 gene by activation of a ubiquitously expressed CreER after the neonatal period leads to a loss of ODAs, the absence of MCC, and chronic rhinosinusitis in the absence of hydrocephalus. These features are consistent with the disease phenotype in patients with PCD who have mutations in the human homolog of *Dnaic1*, demonstrating that our murine model successfully reproduces key aspects of the human disease *in vivo*. *In vitro*, the deletion of *Dnaic1* by tamoxifen treatment of undifferentiated cultures was highly efficient and will provide an essentially unlimited supply of PCD cells for further studies, including studies testing the ability of gene therapy vectors to correct the genetic defect in PCD and restore ciliary activity.

Because the animals in these studies were typically 6 to 10 weeks old at the time of tamoxifen treatment, they already possessed a full complement of active cilia. Although the deletion of *Dnaic1* at the genomic level occurs relatively quickly, as evidenced by PCR analysis of genomic tail DNA several days after treatment, it is not known how long the already formed cilia and ciliated cells remain functional. Our data show that MCC is reduced in the nasopharynx 1 month after the completion of tamoxifen treatment and is completely eliminated by 3 months. The one animal examined at 2 months that maintained approximately 20% of the normal rate of MCC had no evidence of mucus accumulation in the nasal cavity. Quantitative PCR demonstrated that this animal had approximately 20% intact *Dnaic1* remaining after tamoxifen treatment (animal #494; Table E2), suggesting that even a low level of MCC is sufficient to prevent the chronic rhinosinusitis observed in animals with no MCC. In the trachea, MCC was still apparent at 3 months, with one animal maintaining some clearance at 6 months. These data suggest that the turnover rate of ciliary proteins or ciliated cells is faster in the upper airways of mice, possibly due to the greater exposure of these cells to environmental insults. This is consistent with a previous study that demonstrated ciliated cells in the lower airways had a half-life that was significantly longer than those in the trachea (36), although this study did not investigate the turnover of ciliated cells of the upper airways. Our model will allow detailed study of the turnover of ciliary proteins, which may have important implications for therapy. For example, many of the mutations in patients with PCD result in premature termination of translation, and recently drugs have been introduced that promote read-through of these mutations and allow the production of some full-length protein (37, 38). It is not known if these agents can restore ciliary activity to already assembled axonemes.

To avoid the 3 to 6 months required for ciliary turnover and to develop PCD animals more quickly, it may be possible to use an alternative CreER to target specific tissues and avoid expression in the brain. However, our initial goal was to induce the deletion in all tissues to more closely replicate the human disease. We also wanted to test the hypothesis that deletion of *Dnaic1* after the neonatal period would not cause hydrocephalus. In these studies, we observed no evidence of hydrocephalus in animals that were studied up to 11 months after tamoxifen treatment. This result strengthens the hypothesis that the activity of ependymal cilia is important to maintain patency of the aqueduct during early postnatal brain development but may not be essential in the adult animal (17). Similarly, we did not observe histologic evidence of otitis media in *Dnaic1*$^{flox/flox}$ animals treated with tamoxifen (n = 7), perhaps because the deletion of Dnaic1 in our model occurred in older animals. Although otitis media is a common feature of human PCD, it has not been consistently reported to occur in mouse models of PCD.

In addition to the time required for ciliary turnover, the use of an alternative Cre line would be preferable for other reasons. In our initial studies, we observed toxic effects of the Cre transgene when animals were treated with tamoxifen at younger ages or received more frequent treatment. These animals developed intestinal lesions, and some died, possibly due to nonspecific, Cre-mediated DNA damage in the rapidly proliferating intestinal epithelium. In addition, the Rosa/CreER displayed some activity in the absence of tamoxifen treatment, so that in some litters we observed animals with "spontaneous" deletion of the targeted alleles. This occasionally resulted in the birth of homozygous *Dnaic1* null animals; these animals were invariably runted, showed evidence of hydrocephalus, and several displayed situs inversus at necropsy. The use of the more tightly regulated $CreER^{T2}$ or a tissue-specific promoter may alleviate these problems.

Chronic rhinosinusitis is one of the most common symptoms of PCD and is the cause of significant morbidity in the general population. In our studies, 100% of the mice with no MCC in the nasopharynx developed rhinosinusitis, with mucus accumulation, infiltrating neutrophils, and epithelial degeneration. Mucus accumulation was observed predominantly in the dorsal meatus and the adjacent ethmoturbinates, but mucus was also observed adjacent to the nasal septum and in the maxillary sinuses. Other investigators have reported similar findings in other mouse lines with deletions of ciliary genes (12–14, 39); together, these studies demonstrate the importance of normal ciliary activity to the upper (nasal) airways of the mouse. Recent studies have also demonstrated impaired ciliary activity in studies of humans with chronic rhinosinusitis (40, 41).

In contrast, animals with no measurable MCC in their lower airways (trachea) showed no evidence of pulmonary disease for periods up to 11 months after tamoxifen treatment. This is also consistent with the lack of a reported lower airway phenotype in other mouse models with dysfunctional cilia (e.g., Refs. 11–13), although because the *Dnaic1*$^{flox/flox}$ mice did not develop hydrocephalus, our studies were of a significantly longer duration. The lack of a disease phenotype in the lower airways suggests that mice are able to clear secreted mucus and inhaled pathogens sufficiently by means other than MCC to prevent accumulation and subsequent disease. One alternative mechanism that has been proposed to aid in airway clearance is gas–liquid pumping (42, 43), and our mouse model should provide an ideal system for determining the importance of this mechanism. Because of the complex architecture of the nasal turbinates and the limited airflow through the sinuses, gas–liquid pumping may be insufficient to clear mucus from these regions. Another reason that animals with no MCC did not develop significant pulmonary disease in this study may be because laboratory animals are housed in facilities that minimize spontaneous exposure to pathogens. Under conditions of limited exposure to bacterial pathogens, it is likely that the mouse immune system is more than sufficient to prevent lung infection. We observed no evidence of bacterial infection in these studies, even in mice with severe mucus accumulation in the nasal cavity. Controlled challenges with increasing doses of bacteria delivered directly to the lower airways of tamoxifen-treated *Dnaic1*$^{flox/flox}$ animals would be expected to result in more severe or prolonged disease than in control animals, and future studies will test this hypothesis.

In summary, we have developed and characterized a mouse model for PCD that avoids the development of hydrocephalus that frequently occurs when ciliary genes are disrupted. We have also developed methods for quantitatively measuring MCC *in vivo* in the upper and lower airways under conditions in which the airway being studied remains intact and little or no exogenous fluid is added. These studies have demonstrated that the loss of MCC and the apparent turnover of ciliated cells occur more slowly in the lower airways than in the nasopharynx. Tamoxifen-treated *Dnaic1*$^{flox/flox}$ animals reproduce several features of human PCD, including an absence of ODAs in airway cilia examined by electron microscopy, an absence of MCC in the nasopharynx and trachea, and the development of severe rhinosinusitis. This model will be useful for studies of the pathogenesis and treatment of PCD and chronic rhinosinusitis and for studies of airway clearance and respiratory cilia. The inducible inactivation of *Dnaic1* may provide a tool for investigations into other cilia related disorders, including hydrocephalus, congenital heart defects, and infertility.

Conflict of Interest Statement: None of the authors has a financial relationship with a commercial entity that has an interest in the subject of this manuscript.

Acknowledgments: The authors thank Kim Burns and Donald Joyner of the UNC Cystic Fibrosis Center Histology Core for excellent histology and electron microscopy support, Drs. Bill Davis, and Patrick Sears for technical assistance with the ciliary activity measurements, Eileen O'Toole for assistance with the image averaging of ciliary axonemes, Dr. Randy Thresher of the UNC Animal Models Core and Chanwen Sun of the UNC CF Molecular Core for assistance in generating the *Dnaic1*^{flox} mouse, Rob Wonsettler for assistance with cell culture and ciliary activity measurements, and Neal Kramarcy of the UNC Hooker Microscopy Core Facility for microscopy assistance.

References

1. Wanner A, Salathe M, O'Riordan TG. Mucociliary clearance in the airways. *Am J Respir Crit Care Med* 1996;154:1868–1902.
2. Knowles MR, Boucher RC. Mucus clearance as a primary innate defense mechanism for mammalian airways. *J Clin Invest* 2002;109: 571–577.
3. Leigh MW. Primary ciliary dyskinesia. In: Chernick V, Boat TF, editors. Disorders of the respiratory tract of children. 6 ed. Philadelphia, PA: W.B. Saunders; 1998. pp. 819–825.
4. Kennedy MP, Ostrowski LE. Primary ciliary dyskinesia and upper airway diseases. *Curr Allergy Asthma Rep* 2006;6:513–517.
5. Noone PG, Leigh MW, Sannuti A, Minnix SL, Carson JL, Hazucha M, Zariwala MA, Knowles MR. Primary ciliary dyskinesia: diagnostic and phenotypic features. *Am J Respir Crit Care Med* 2004;169: 459–467.
6. Meeks M, Bush A. Primary ciliary dyskinesia (PCD). *Pediatr Pulmonol* 2000;29:307–316.
7. Boucher RC. Evidence for airway surface dehydration as the initiating event in CF airway disease. *J Intern Med* 2007;261:5–16.
8. Boucher RC. New concepts of the pathogenesis of cystic fibrosis lung disease. *Eur Respir J* 2004;23:146–158.
9. Chen J, Knowles HJ, Hebert JL, Hackett BP. Mutation of the mouse hepatocyte nuclear factor/forkhead homologue 4 gene results in an absence of cilia and random left-right asymmetry. *J Clin Invest* 1998; 102:1077–1082.
10. Brody SL, Yan XH, Wuerffel MK, Song SK, Shapiro SD. Ciliogenesis and left-right axis defects in forkhead factor HFH-4-null mice. *Am J Respir Cell Mol Biol* 2000;23:45–51.
11. Tanaka H, Iguchi N, Toyama Y, Kitamura K, Takahashi T, Kaseda K, Maekawa M, Nishimune Y. Mice deficient in the axonemal protein Tektin-t exhibit male infertility and immotile-cilium syndrome due to impaired inner arm dynein function. *Mol Cell Biol* 2004;24:7958–7964.
12. Ibanez-Tallon I, Gorokhova S, Heintz N. Loss of function of axonemal dynein Mdnah5 causes primary ciliary dyskinesia and hydrocephalus. *Hum Mol Genet* 2002;11:715–721.
13. Lee L, Campagna DR, Pinkus JL, Mulhern H, Wyatt TA, Sisson JH, Pavlik JA, Pinkus GS, Fleming MD. Primary ciliary dyskinesia in mice lacking the novel ciliary protein Pcdp1. *Mol Cell Biol* 2008;28: 949–957.
14. Fernandez-Gonzalez A, Kourembanas S, Wyatt TA, Mitsialis SA. Mutation of murine adenylate kinase 7 underlies a primary ciliary dyskinesia phenotype. *Am J Respir Cell Mol Biol* 2009;40:305–313.
15. Tan SY, Rosenthal J, Zhao XQ, Francis RJ, Chatterjee B, Sabol SL, Linask KL, Bracero L, Connelly PS, Daniels MP, *et al.* Heterotaxy and complex structural heart defects in a mutant mouse model of primary ciliary dyskinesia. *J Clin Invest* 2007;117:3742–3752.
16. Zariwala M, O'Neal WK, Noone PG, Leigh MW, Knowles MR, Ostrowski LE. Investigation of the possible role of a novel gene,

DPCD, in primary ciliary dyskinesia. *Am J Respir Cell Mol Biol* 2004; 30:428–434.
17. Ibanez-Tallon I, Pagenstecher A, Fliegauf M, Olbrich H, Kispert A, Ketelsen UP, North A, Heintz N, Omran H. Dysfunction of axonemal dynein heavy chain Mdnah5 inhibits ependymal flow and reveals a novel mechanism for hydrocephalus formation. *Hum Mol Genet* 2004;13:2133–2141.
18. Zariwala M, Noone PG, Sannuti A, Minnix S, Zhou Z, Leigh MW, Hazucha M, Carson JL, Knowles MR. Germline mutations in an intermediate chain dynein cause primary ciliary dyskinesia. *Am J Respir Cell Mol Biol* 2001;25:577–583.
19. Zariwala MA, Leigh MW, Ceppa F, Kennedy MP, Noone PG, Carson JL, Hazucha MJ, Lori A, Horvath J, Olbrich H, *et al.* Mutations of DNAI1 in primary ciliary dyskinesia: evidence of founder effect in a common mutation. *Am J Respir Crit Care Med* 2006;174:858–866.
20. Pennarun G, Escudier E, Chapelin C, Bridoux AM, Cacheux V, Roger G, Clement A, Goossens M, Amselem S, Duriez B. Loss-of-function mutations in a human gene related to *Chlamydomonas reinhardtii* dynein IC78 result in primary ciliary dyskinesia. *Am J Hum Genet* 1999;65:1508–1519.
21. Guichard C, Harricane MC, Lafitte JJ, Godard P, Zaegel M, Tack V, Lalau G, Bouvagnet P. Axonemal dynein intermediate-chain gene (DNAI1) mutations result in situs inversus and primary ciliary dyskinesia (Kartagener syndrome). *Am J Hum Genet* 2001;68:1030–1035.
22. Badea TC, Wang Y, Nathans J. A noninvasive genetic/pharmacologic strategy for visualizing cell morphology and clonal relationships in the mouse. *J Neurosci* 2003;23:2314–2322.
23. Hayashi S, McMahon AP. Efficient recombination in diverse tissues by a tamoxifen-inducible form of Cre: a tool for temporally regulated gene activation/inactivation in the mouse. *Dev Biol* 2002;244:305–318.
24. You Y, Richer EJ, Huang T, Brody SL. Growth and differentiation of mouse tracheal epithelial cells: selection of a proliferative population. *Am J Physiol Lung Cell Mol Physiol* 2002;283:L1315–L1321.
25. Sisson JH, Stoner JA, Ammons BA, Wyatt TA. All-digital image capture and whole-field analysis of ciliary beat frequency. *J Microsc* 2003;211:103–111.
26. Ostrowski LE, Blackburn K, Radde KM, Moyer MB, Schlatzer DM, Moseley A, Boucher RC. A proteomic analysis of human cilia: identification of novel components. *Mol Cell Proteomics* 2002;1: 451–465.
27. Mall M, Grubb BR, Harkema JR, O'Neal WK, Boucher RC. Increased airway epithelial Na+ absorption produces cystic fibrosis-like lung disease in mice. *Nat Med* 2004;10:487–493.
28. Popesko P, Rajtova V, Horak J. Anatomy of small laboratory animals. Prescott, AZ: Wolfe Publishing LTD; 1992.
29. Zahm JM, Gaillard D, Dupuit F, Hinnrasky J, Porteous D, Dorin JR, Puchelle E. Early alterations in airway mucociliary clearance and inflammation of the lamina propria in CF mice. *Am J Physiol* 1997; 272:C853–C859.
30. Look DC, Walter MJ, Williamson MR, Pang L, You Y, Sreshta JN, Johnson JE, Zander DS, Brody SL. Effects of paramyxoviral infection on airway epithelial cell Foxj1 expression, ciliogenesis, and mucociliary function. *Am J Pathol* 2001;159:2055–2069.
31. Mery S, Gross EA, Joyner DR, Godo M, Morgan KT. Nasal diagrams: a tool for recording the distribution of nasal lesions in rats and mice. *Toxicol Pathol* 1994;22:353–372.
32. O'Toole E, Mastronarde D, McIntosh JR, Porter ME. Computer-assisted analysis of flagellar structure. *Methods Cell Biol* 1995;47:183–191.
33. Wilkerson CG, King SM, Koutoulis A, Pazour GJ, Witman GB. The 78,000 M(r) intermediate chain of Chlamydomonas outer arm dynein is a WD-repeat protein required for arm assembly. *J Cell Biol* 1995; 129:169–178.
34. Harkema JR, Carey SA, Wagner JG. The nose revisited: a brief review of the comparative structure, function, and toxicologic pathology of the nasal epithelium. *Toxicol Pathol* 2006;34:252–269.
35. Cavrenne R, De Busscher V, Bolen G, Billen F, Clercx C, Snaps F. Primary ciliary dyskinesia and situs inversus in a young dog. *Vet Rec* 2008;163:54–55.
36. Rawlins EL, Hogan BL. Ciliated epithelial cell lifespan in the mouse trachea and lung. *Am J Physiol Lung Cell Mol Physiol* 2008;295: L231–L234.
37. Du M, Liu X, Welch EM, Hirawat S, Peltz SW, Bedwell DM. PTC124 is an orally bioavailable compound that promotes suppression of the human CFTR-G542X nonsense allele in a CF mouse model. *Proc Natl Acad Sci USA* 2008;105:2064–2069.
38. Kerem E, Hirawat S, Armoni S, Yaakov Y, Shoseyov D, Cohen M, Nissim-Rafinia M, Blau H, Rivlin J, Aviram M, *et al.* Effectiveness of PTC124 treatment of cystic fibrosis caused by nonsense mutations: a prospective phase II trial. *Lancet* 2008;372:719–727.
39. Kobayashi Y, Watanabe M, Okada Y, Sawa H, Takai H, Nakanishi M, Kawase Y, Suzuki H, Nagashima K, Ikeda K, *et al.* Hydrocephalus, situs inversus, chronic sinusitis, and male infertility in DNA polymerase lambda-deficient mice: possible implication for the pathogenesis of immotile cilia syndrome. *Mol Cell Biol* 2002;22:2769–2776.
40. Baroody FM. Mucociliary transport in chronic rhinosinusitis. *Clin Allergy Immunol* 2007;20:103–119.
41. Chen B, Shaari J, Claire SE, Palmer JN, Chiu AG, Kennedy DW, Cohen NA. Altered sinonasal ciliary dynamics in chronic rhinosinusitis. *Am J Rhinol* 2006;20:325–329.
42. Benjamin RG, Chapman GA, Kim CS, Sackner MA. Removal of bronchial secretions by two-phase gas-liquid transport. *Chest* 1989; 95:658–663.
43. Kim CS, Rodriguez CR, Eldridge MA, Sackner MA. Criteria for mucus transport in the airways by two-phase gas-liquid flow mechanism. *J Appl Physiol* 1986;60:901–907.